AMERICAN SOCIETY FOR MICROBIOLOGY | Infection and Immunity®

MOLECULAR PATHOGENESIS

The VirAB ABC Transporter Is Required for VirR Regulation of *Listeria monocytogenes* Virulence and Resistance to Nisin

Daniel Grubaugh,[a] James M. Regeimbal,[a]* Pallab Ghosh,[a] Yan Zhou,[a] Peter Lauer,[b] Thomas W. Dubensky, Jr.,[b] Darren E. Higgins[a]

[a]Department of Microbiology and Immunobiology, Harvard Medical School, Boston, Massachusetts, USA
[b]Aduro Biotech, Berkeley, California, USA

ABSTRACT *Listeria monocytogenes* is a Gram-positive intracellular pathogen that causes a severe invasive disease. Upon infecting a host cell, *L. monocytogenes* upregulates the transcription of numerous factors necessary for productive infection. VirR is the response regulator component of a two-component regulatory system in *L. monocytogenes*. In this report, we have identified the putative ABC transporter encoded by genes *lmo1746-lmo1747* as necessary for VirR function. We have designated *lmo1746-lmo1747 virAB*. We constructed an in-frame deletion of *virAB* and determined that the Δ*virAB* mutant exhibited reduced transcription of VirR-regulated genes. The Δ*virAB* mutant also showed defects in *in vitro* plaque formation and *in vivo* virulence that were similar to those of a Δ*virR* deletion mutant. Since VirR is important for innate resistance to antimicrobial agents, we determined the MICs of nisin and bacitracin for Δ*virAB* bacteria. We found that VirAB expression was necessary for nisin resistance but was dispensable for resistance to bacitracin. This result suggested a VirAB-independent mechanism of VirR regulation in response to bacitracin. Lastly, we found that the Δ*virR* and Δ*virAB* mutants had no deficiency in growth in broth culture, intracellular replication, or production of the ActA surface protein, which facilitates actin-based motility and cell-to-cell spread. However, the Δ*virR* and Δ*virAB* mutants produced shorter actin tails during intracellular infection, which suggested that these mutants have a reduced ability to move and spread via actin-based motility. These findings have demonstrated that *L. monocytogenes* VirAB functions in a pathway with VirR to regulate the expression of genes necessary for virulence and resistance to antimicrobial agents.

KEYWORDS *Listeria monocytogenes*, *virABRS*, virulence regulation, intracellular infection, antimicrobial resistance

Listeria monocytogenes is a Gram-positive bacterium commonly found in the soil. *L. monocytogenes* is also a facultatively intracellular pathogen that can infect humans through the ingestion of contaminated foods. Infections by *L. monocytogenes* can lead to listeriosis, a severe invasive disease that can be life-threatening. In untreated cases of listeriosis, *L. monocytogenes* can spread to distal organs, such as the brain or the placenta, leading to meningoencephalitis or septic abortion (1). During the infection of a mammalian host, *L. monocytogenes* alters the expression of numerous genes, downregulating factors that are important for environmental growth, such as flagellin, and upregulating many virulence factors that are necessary for host cell invasion and intracellular growth (2, 3). Four transcriptional regulators have been shown to control virulence in *L. monocytogenes*: PrfA, σ^B, CodY, and VirR. PrfA is the central virulence regulator for *L. monocytogenes* pathogenesis (4). PrfA activates the transcription of critical virulence factors, including the pore-forming cytolysin listeriolysin O (LLO), which allows *L. monocytogenes* to escape the host phagosome and enter the cytosol,

Received 8 December 2017 **Accepted** 17 December 2017

Accepted manuscript posted online 20 December 2017

Citation Grubaugh D, Regeimbal JM, Ghosh P, Zhou Y, Lauer P, Dubensky TW, Jr, Higgins DE. 2018. The VirAB ABC transporter is required for VirR regulation of *Listeria monocytogenes* virulence and resistance to nisin. Infect Immun 86:e00901-17. https://doi.org/10.1128/IAI.00901-17.

Editor Nancy E. Freitag, University of Illinois at Chicago

Address correspondence to Darren E. Higgins, darren_higgins@hms.harvard.edu.

* Present address: James M. Regeimbal, Naval Medical Research Center, Silver Spring, Maryland, USA.

and the actin motility-inducing surface protein ActA, which allows *L. monocytogenes* to spread from cell to cell without encountering the extracellular milieu (5). σ^B is an alternative sigma factor that regulates *L. monocytogenes* gene expression in response to stress. Gene regulation by σ^B interacts with that by PrfA and has been shown to be important for virulence (3, 6). CodY is a transcriptional regulator that activates the transcription of *prfA* and other genes in response to low concentrations of branched-chain amino acids found inside host cells (7, 8). Of these transcriptional regulators, VirR is the least characterized.

VirR is the response regulator component of a two-component system (TCS) (9). A TCS consists of a sensor histidine kinase and a response regulator that are generally cotranscribed (10). Most sensor histidine kinases contain an extracellular sensing domain that binds a product outside the bacterial cell. When this receptor is engaged, the sensor kinase phosphorylates a histidine residue on its kinase core domain. The response regulator then engages this phosphorylated residue and acts as a phosphatase to transfer the phosphate to itself. The response regulator then undergoes a conformational shift that allows it to perform downstream functions, often acting as a transcription factor to modify the expression of genes within its regulon (11). VirR was initially discovered in a transposon mutagenesis screen to identify *L. monocytogenes* mutants that exhibited reduced virulence in a mouse model of infection. That study also identified VirS as the cognate sensor kinase for VirR and used microarray analysis to establish the VirR transcriptional regulon (9). The expression of VirR and that of many of the VirR-regulated genes are strongly induced during *in vivo* infection, suggesting that VirR is involved in the sensing of the host cell environment by *L. monocytogenes* (12). In general, VirR has been shown to regulate the transcription of genes that are involved in defense against cell envelope stress. Among the most highly VirR regulated genes is the *dltABCD* operon, the products of which are responsible for incorporating D-alanine into lipoteichoic acid, a modification that helps counteract cationic antimicrobial peptides (CAMPs) by increasing the overall cell surface charge (13, 14). Other VirR-regulated factors include MprF, a protein that lysinylates phospholipids in the *L. monocytogenes* cell membrane to prevent CAMP binding (15), and AnrAB, an ATP-binding cassette (ABC) transporter believed to be involved in the detoxification of antimicrobials (16). Furthermore, mutants of VirR have been shown to be sensitive to several cell envelope-targeting antimicrobials, including those used in food preservation (17). It has been shown through sequence analysis that VirR belongs to a family of homologous TCSs, typified by *Bacillus subtilis* BceRS (18), which are conserved throughout the phylum *Firmicutes* (19, 20). The sensor kinases of these TCSs lack the extracellular sensor domains that would generally be used for engaging a ligand. Instead, it has been shown that ligand sensing is accomplished by an ABC transporter that is generally encoded by genes located close to the associated TCS genes in the genome. The ABC transporter in these systems forms a cell-surface complex that activates the sensor kinase, causing phosphorylation of the response regulator (21, 22). Thus, the expression of genes regulated by the response regulator is dependent upon the action of the ABC transporter (23). It has been proposed that VirR signaling functions in this manner (19), but the involvement of an ABC transporter in VirR signaling has yet to be shown.

Recently, the *L. monocytogenes* strains most commonly used for virulence studies were compared for differences in general genetic and virulence characteristics (24). That study showed that the commonly used *L. monocytogenes* strain EGD, the only *L. monocytogenes* strain used to date for studies of the role of VirR in *L. monocytogenes* virulence, contains a mutation in the *prfA* gene. The authors demonstrated that this mutation led to a PrfA protein that was constitutively activated (PrfA*). As a consequence, many *L. monocytogenes* virulence factors in the EGD strain were expressed at high levels regardless of whether the bacteria were actively infecting host cells. Since we were interested in the role of VirR for host sensing and virulence, we performed additional studies on VirR using *L. monocytogenes* strain 10403S, a widely used strain of *L. monocytogenes* that does not harbor a PrfA* mutation. Here, we describe a VirR-associated ABC transporter that we have designated VirAB. We demonstrate that the

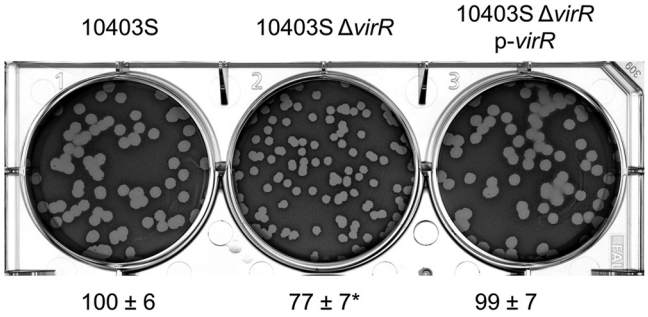

FIG 1 Plaque formation by *L. monocytogenes* 10403S-derived strains. L2 murine fibroblasts were infected with approximately 5×10^4 CFU of the indicated strains. The infected cells were washed and were overlaid with 0.7% agarose in DMEM containing gentamicin. Seventy-two hours later, cultured cells were stained with neutral red to allow for the visualization of plaques. Wells were photographed, and plaque sizes (diameters) were measured using Adobe Photoshop. Images are representative of the plaque sizes observed. The plaque size of each strain is given below the image as a percentage of the plaque size of 10403S and represents the average ± standard deviation from three independent experiments measuring >10 plaques/experiment. The asterisk indicates a significant difference ($P < 0.001$) from 10403S as determined by one-way ANOVA with a *post hoc* Dunnett multiple-comparison test.

VirAB transporter, similarly to VirR, is necessary for *L. monocytogenes* virulence and that VirAB contributes to a previously underappreciated role of VirR for the cell-to-cell spread of *L. monocytogenes* during intracellular infection.

RESULTS

10403S Δ*virR* is deficient in plaque formation. We initially sought to determine the virulence characteristics of a Δ*virR* mutant of an *L. monocytogenes* strain lacking a PrfA* mutation. To this end, we generated an in-frame deletion mutant of the *virR* gene within *L. monocytogenes* 10403S and used the Δ*virR* deletion mutant strain to perform plaquing assays in L2 mouse fibroblasts. The 10403S Δ*virR* strain produced plaques that averaged 77% of the diameter of those produced by the parental strain 10403S, indicating a potential defect in intracellular growth or cell-to-cell spread (Fig. 1). The 10403S Δ*virR* plaquing defect could be complemented by expressing VirR from the p-*virR* vector integrated at the $tRNA^{Arg}$ phage integration site. This observation is in contrast to previous studies of the VirR response regulator, which showed no defect in intracellular growth or actin tail formation for a Δ*virR* mutant (9). However, since those studies used an *L. monocytogenes* EGD-derived Δ*virR* mutant, it is likely that any role of VirR in cell-to-cell spread would have gone undetected due to the PrfA*-mediated overproduction of virulence factors, including ActA and LLO, within the mutant strain.

Delineation of the VirR regulon. Since deficiencies in plaque formation are often attributable to misregulation of key *L. monocytogenes* virulence factors, we hypothesized that the 10403S Δ*virR* plaquing phenotype may be due to a previously unrecognized role of VirR in the transcriptional regulation of *L. monocytogenes* virulence determinants. To investigate this hypothesis, we performed RNA sequencing (RNA-seq) on RNA extracted from 10403S and the 10403S Δ*virR* mutant grown in LB broth. We did not observe any effects of *virR* deletion on the transcription of PrfA-regulated genes. Indeed, the VirR regulon that we identified in 10403S was very similar to the published regulon identified in EGD (Table 1). As shown previously, genes involved in resistance to cationic antimicrobials, including the *dltABCD* operon, the *anrAB* ABC transporter, and the *mprF* gene, were transcriptionally downregulated in strain 10403S Δ*virR*. Also in agreement with previously published data, the small hypothetical proteins encoded by *lmo0604*, *lmo2156*, and *lmo2177* were among the most strongly differentially regulated transcripts in the Δ*virR* mutant strain. In addition to identifying these previously known elements of the VirR regulon, we identified six loci that were not previously reported as differentially expressed in the absence of VirR (9). Most prominent among these was the Rli32 (*lmos24*) small RNA (sRNA), whose transcription was downregulated >70-fold in the 10403S Δ*virR* mutant. The involvement of an sRNA in the VirR regulon

TABLE 1 Genes significantly differentially regulated at least 2-fold in 10403S Δ*virR* relative to expression in 10403S

Gene or locus[a]	Description	Fold change	*P* value (FDR corrected)
dltA	D-Alanylation of teichoic acid	−64.68	3.55×10^{-234}
dltB	D-Alanylation of teichoic acid	−72.29	9.88×10^{-211}
dltC	D-Alanylation of teichoic acid	−78.31	5.98×10^{-216}
dltD	D-Alanylation of teichoic acid	−62.55	1.34×10^{-228}
lmo0325	Transcriptional regulator	−4.09	1.76×10^{-13}
lmo0604	Predicted protein	−28.23	4.13×10^{-42}
lmo0791	Predicted protein	2	8.12×10^{-09}
lmo0833	Hypothetical protein	−6.65	6.56×10^{-10}
mprF	Lysinylation of phospholipids	−2.07	1.39×10^{-12}
lmo1744	NAD-dependent epimerase-like protein	2.3	1.24×10^{-09}
anrA	ABC transporter	−52.05	3.62×10^{-156}
anrB	ABC transporter	−51.23	1.19×10^{-91}
lmo2156	Hypothetical protein	−194.23	5.14×10^{-146}
lmo2177	Hypothetical membrane protein	−23.49	1.31×10^{-160}
lmo2439	Hypothetical protein	−4.76	4.63×10^{-30}
lmo2708	PTS transporter subunit	4.03	7.55×10^{-03}
Rli32 sRNA	Small RNA	−74.61	1.72×10^{-110}

[a]Boldface gene or locus names indicate features previously shown to be regulated by VirR.

is of interest, since sRNAs similar to the Rli32 sRNA have been shown to have effects on the posttranscriptional regulation of *L. monocytogenes* gene product expression (25, 26). Any VirR-mediated changes in *L. monocytogenes* gene expression that occurred posttranscriptionally through the action of the Rli32 sRNA would not have been identified in our RNA-seq analysis. We also identified two small hypothetical open reading frames (ORFs), *lmo0833* and *lmo0325*, that were transcriptionally downregulated 7- and 4-fold, respectively, in 10403S Δ*virR*. Furthermore, we found small but significant increases in the transcription of the predicted ORF *lmo0791* and of the pentose phosphate transporter subunit encoded by *lmo2708*.

In contrast to the previous report on the VirR regulon in strain EGD (9), we did not observe transcriptional downregulation of the downstream genes in the *virR* operon, including *virS*. We believe that this discrepancy may arise from polar effects of the *virR*::Tn*917* transposon insertion strain that was used for the microarray analysis in that study (9). However, we did observe a small (2-fold) increase in the transcription of *lmo1744* and a significant but <2-fold increase in the transcription of *lmo1743*. The *lmo1744* locus is annotated as a hypothetical NAD-dependent epimerase, but its function has not been directly studied. Interestingly, the operon encoding GraRS, the *Staphylococcus aureus* homologues of VirRS, contains *graX*, encoding a protein that was initially annotated as an NAD-dependent epimerase but has since been shown to be involved in signal transduction between the sensor ABC transporter VraFG and the GraS kinase (21).

The *L. monocytogenes virR* operon structure is of interest, since many of the genes in the operon share significant sequence similarity with genes involved in VirR homologue signaling in other *Firmicutes* species (Fig. 2). Some of the best studied of these systems are the BceRS system of *Bacillus subtilis* (18) and the GraXRS system of *Staphylococcus aureus* (21). Like the VirRS system, these TCSs are involved in cell envelope stress and resistance to antimicrobial agents. Like VirS, BceS and GraS lack the large extracellular loop that many TCS sensor kinases use for substrate binding. Instead, the sensor kinases in these systems bind to and sense through the associated ABC transporters: BceAB in *B. subtilis* and VraFG in *S. aureus*. *L. monocytogenes* has two ABC transporters with significant sequence homology to these proteins: AnrAB and the putative transporter encoded by *lmo1746-lmo1747*. Previous studies have identified *lm.G_1771*, an ABC transporter permease in *L. monocytogenes* serotype 4b strain G that is identical to *lmo1746*, and found that *lm.G_1771* had a role in the regulation of biofilm formation (27, 28). Further microarray analyses indicated that the product of *lm.G_1771* regulates the transcription of *anrAB* and *dltABCD*, members of the VirR regulon (29).

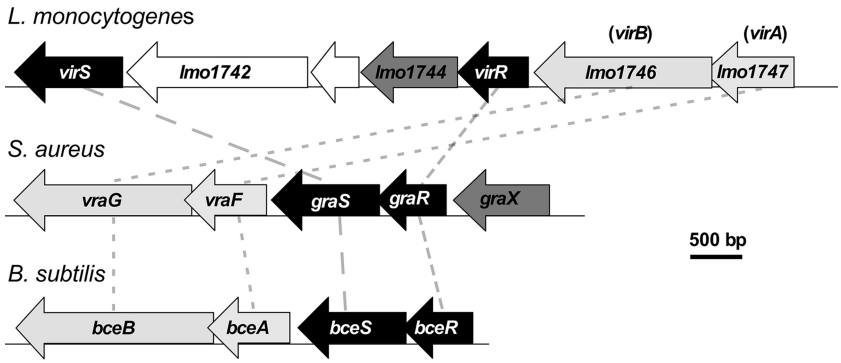

FIG 2 Schematic representation of the *L. monocytogenes virR* genetic locus and its homologues in other *Firmicutes* bacteria. Dashed lines indicate genes that are homologous across species. Filled arrows, histidine kinase and response regulator genes; light shaded arrows, ABC transporter genes; dark shaded arrow, NAD-dependent epimerase-like gene; open arrows, genes with unknown function in TCS signaling. All genes are represented to scale. Proposed gene names are shown in parentheses.

However, the characteristics of this regulation are different from what has been observed for VirR. Specifically, while deletion of *virR* in 10403S and EGD resulted in strong downregulation of *dltABCD* and *anrAB* transcription, the *lm.G_1771* deletion resulted in the downregulation of *dltABCD* but upregulation of *anrAB*. Despite these strain differences, we hypothesized that the transporter encoded by *lmo1746-lmo1747* is fulfilling a signaling role for VirRS, and we have proposed the name VirAB for this *L. monocytogenes* ABC transporter (Fig. 2).

VirAB is required for the transcription of VirR-regulated genes. If VirAB is necessary for VirR signaling, then VirR-regulated genes should be transcriptionally downregulated in the absence of the VirAB transporter. Thus, we generated an in-frame deletion mutant of the 10403S *virAB* genes. We then isolated RNA from *L. monocytogenes* 10403S and the Δ*virR* and Δ*virAB* mutants that had been grown to exponential phase in broth culture. Quantitative reverse transcription-PCR (qRT-PCR) was then used to quantify the relative mRNA levels of the highly VirR regulated genes *anrB* and *dltD* and of the Rli32 small RNA. We found that *anrB* transcript levels were almost 10-fold reduced in the Δ*virR* and Δ*virAB* mutant strains from that in 10403S (Fig. 3A). *dltD* transcript levels were >10-fold lower in the Δ*virR* strain than in 10403S and were also significantly reduced in the Δ*virAB* strain (3.5-fold lower than in 10403S), albeit not as much as for the Δ*virR* mutant (Fig. 3B). Transcription of the Rli32 small RNA was strongly impaired in both the Δ*virR* and Δ*virAB* mutant strains relative to that in 10403S (Fig. 3C). Taken together, these data show that VirAB is necessary for the transcription of VirR-regulated genes.

Deletion of the *virB* paralogue in *L. monocytogenes* 4b strain G has been shown to lead to an increase in *srtA* mRNA levels (29). However, we did not observe an effect on *srtA* transcription in the 10403S Δ*virR* strain by RNA-seq. To determine if this reflects a difference in the regulons of VirAB and VirR, we used qRT-PCR to measure *srtA* mRNA levels in 10403S and the 10403S-derived Δ*virR* and Δ*virAB* strains. We found no significant difference in *srtA* transcription between either mutant and 10403S (Fig. 3D). This dissimilarity with the previous study may reflect strain differences or differential regulation of VirR-controlled genes during exponential-phase growth relative to biofilm-forming conditions.

The 10403S Δ*virAB* mutant exhibits a plaquing defect similar to that of the 10403S Δ*virR* mutant. To investigate a potential role of VirAB in *L. monocytogenes* pathogenesis, we initially performed plaquing assays in cultured L2 fibroblasts. We found that the Δ*virAB* mutant had a plaque diameter 26% lower than that of 10403S, a defect similar to that of the Δ*virR* strain (Table 2). This defect could be complemented by expressing VirAB in *trans* from the integrated p-*virAB* vector. Overexpression of TCS response regulators, including the VirR orthologue BceR, has been shown to lead to

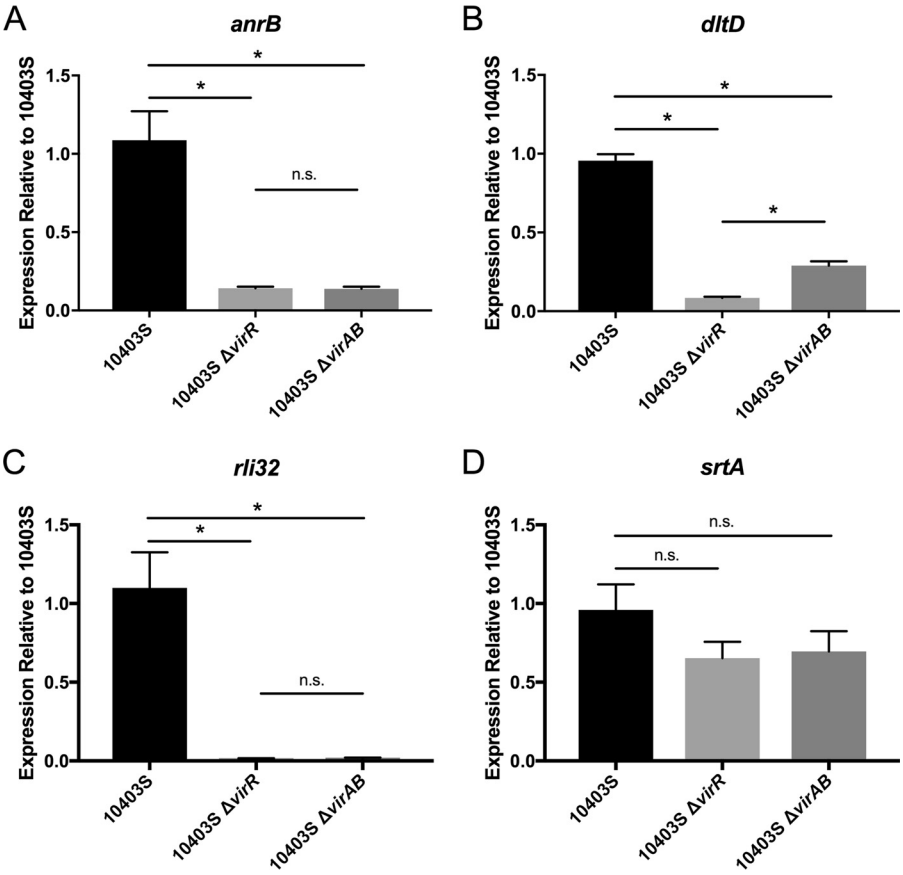

FIG 3 Quantification of VirR-regulated gene transcription. RNA was isolated from cultures of 10403S, 10403S Δ*virR*, and 10403S Δ*virAB*. Primers specific for *anrB* (A), *dltD* (B), the Rli32 sRNA (C), and *srtA* (D) were used to perform quantitative reverse transcription-PCR on cDNA generated from the isolated RNA. Relative quantification of mRNA levels was achieved using the $\Delta\Delta C_T$ method normalized to 16S rRNA, and the amplification factor for each set of primers was corrected for measured primer efficiency. Data are averages of three biological replicates; error bars, standard deviations. Significance was determined by one-way ANOVA with a *post hoc* Dunnett multiple-comparison test. *, $P < 0.0001$; n.s., no significant difference ($P > 0.05$).

constitutive expression of downstream genes, even in the absence of the sensor kinase (18). Thus, we overexpressed VirR in the Δ*virAB* mutant using the pLOV integration vector (30). We found that overexpression of VirR in the Δ*virAB* pLOV::*virR* strain complemented the Δ*virAB* mutant plaquing phenotype (plaque diameter, 95% of that in 10403S). We also produced an in-frame triple mutant spanning the *virABR* genes. This strain demonstrated a plaquing defect similar (21%) to those of the individual Δ*virAB* and Δ*virR* strains (Table 2). Taken together, these data show that VirAB is necessary for

TABLE 2 Plaque formation by 10403S-derived strains

Strain	Plaque diam ± SD[a]
10403S	100 ± 6
10403S Δ*virR*	77 ± 7[b]
10403S Δ*virR* p-*virR*	99 ± 7
10403S Δ*virAB*	74 ± 5[b]
10403S Δ*virAB* p-*virAB*	98 ± 6
10403S Δ*virAB* pLOV::*virR*	95 ± 7[b]
10403S Δ*virABR*	79 ± 7[b]

[a]Expressed as a percentage of the plaque diameter of 10403S.
[b]Statistically significant difference from 10403S (P, <0.01 by one-way ANOVA with a *post hoc* Dunnett multiple-comparison test).

TABLE 3 MICs of nisin and bacitracin

Strain	Median MIC (μg/ml)	
	Nisin	Bacitracin
10403S	3.12	125
10403S Δ*virR*	0.146[a]	0.49[a]
10403S Δ*virAB*	0.146[a]	62.5
10403S Δ*anrB*	0.146[a]	0.49[a]
10403S Δ*virR* p-*virR*	4.68	125
10403S Δ*virAB* p-*virAB*	3.12	125
10403S Δ*virAB* pLOV::*virR*	6.25	125

[a]Statistically significant difference from 10403S ($P < 0.05$) as determined by a *post hoc* Dunn multiple-comparison test after a Kruskal-Wallis test ($P < 0.0001$).

optimal intracellular infection by *L. monocytogenes* and suggest that VirABR work together in the same signaling pathway.

VirAB is necessary for 10403S resistance to nisin but not to bacitracin. Since VirR and its homologues are known to be involved in cell envelope stress responses and resistance to antimicrobial agents, we determined the MICs of two cationic cell wall-targeting antimicrobial agents: bacitracin and nisin. Both of these antibiotics interfere with peptidoglycan synthesis by binding to the lipid carrier of peptidoglycan subunits. Nisin prevents the export of the loaded lipid II molecule across the bacterial cell membrane (31), while bacitracin inhibits the recycling of the bactoprenol lipid carrier after the delivery of the peptidoglycan subunit (32). We grew *L. monocytogenes* 10403S and the Δ*virR* and Δ*virAB* deletion mutants in media containing serial dilutions of the two antimicrobial agents. We also generated and analyzed an in-frame deletion mutant of the *anrB* gene, since *anrB* is regulated by VirR and has been shown to be critical for the innate resistance of *L. monocytogenes* to both nisin and bacitracin. We found that the growth of the Δ*virR*, Δ*virAB*, and Δ*anrB* deletion strains was inhibited at nisin concentrations approximately 16-fold lower than the MIC for the parental strain 10403S (Table 3). The sensitivity to nisin could be complemented; the nisin MICs for the Δ*virR* p-*virR* and Δ*virAB* p-*virAB* strains were similar to that for 10403S, and the nisin MIC for 10403S Δ*virAB* pLOV::*virR* was 2-fold higher than that for 10403S. Thus, this observation suggests that VirR function is downstream of VirAB in resistance to nisin. In analyzing the MIC of bacitracin, we found that the MIC for the Δ*virR* and Δ*anrB* deletion strains was approximately 255-fold lower than that for 10403S. However, the bacitracin MIC for the Δ*virAB* mutant was only 2-fold lower than that for 10403S, and the difference was not statistically significant (Table 3). These data suggest that while VirAB is critical for *L. monocytogenes* resistance to nisin, it is not required for *L. monocytogenes* resistance to bacitracin.

A high concentration of nisin induces the expression of VirR-regulated genes. While VirR and its regulon have been shown to be necessary for resistance to cationic antimicrobials such as nisin, there is a lack of direct evidence linking the sensing of cationic antimicrobials to VirR activity. In fact, previous work has shown that expression of the VirR-regulated *dlt* operon does not increase in the presence of 0.1 μg/ml nisin (17). To verify this observation in our system, we grew 10403S and the Δ*virR* and Δ*virAB* deletion strains in the presence of two concentrations of nisin (0.1 or 1.0 μg/ml) and used qRT-PCR to measure the expression of the VirR-regulated genes *anrB* and *dltD*.

In keeping with previous studies (17), we found that growth in 0.1 μg/ml nisin had no effect on *anrB* (Fig. 4A) or *dltD* (Fig. 4B) expression. However, when 10403S was grown in 1.0 μg/ml nisin, *anrB* expression increased 6-fold, and *dltD* expression increased 2-fold, over that with growth in BHI medium. However, the Δ*virR* and Δ*virAB* mutant strains were unable to grow at this increased concentration of nisin. These data show that the expression of VirR-controlled genes responds to increased nisin concentrations.

The 10403S Δ*virAB* mutant is attenuated during *in vivo* infection. To determine whether VirAB is necessary for *L. monocytogenes* virulence, we infected BALB/c mice

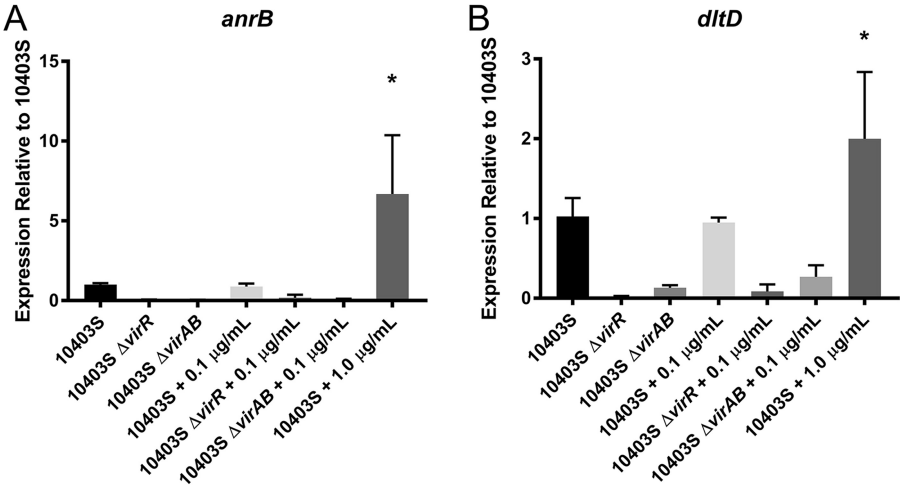

FIG 4 Quantification of VirR-regulated gene transcription in response to nisin. RNA was isolated from cultures of 10403S, 10403S Δ*virR*, and 10403S Δ*virAB* grown in 0.1 or 1.0 μg/ml nisin. Primers specific for *anrB* (A) or *dltD* (B) were used to perform quantitative reverse transcription-PCR on cDNA generated from the isolated RNA. Relative quantification of mRNA levels was achieved using the $\Delta\Delta C_T$ method normalized to 16S rRNA, and the amplification factor for each set of primers was corrected for measured primer efficiency. Data are averages from three biological replicates; error bars indicate standard deviations. Significance was determined by one-way ANOVA with a *post hoc* Dunnett multiple-comparison test. *, $P < 0.001$.

intravenously with 2×10^4 CFU of 10403S or the Δ*virR*, Δ*virAB*, or Δ*virABR* deletion strain. In agreement with previous reports, the Δ*virR* strain was defective in colonization of both the liver and the spleen, exhibiting 33-fold fewer bacteria than the 10403S parental strain in the spleen (Fig. 5A) and 44-fold fewer bacteria in the liver (Fig. 5B). The Δ*virAB* mutant strain exhibited a virulence defect similar to that of 10403S Δ*virR*, with 31-fold fewer bacteria in the spleen and 34-fold fewer bacteria in the liver. The Δ*virABR* triple mutant also exhibited a significant virulence defect, although the median bacterial burdens were higher than those for either the Δ*virR* or the Δ*virAB* deletion strain.

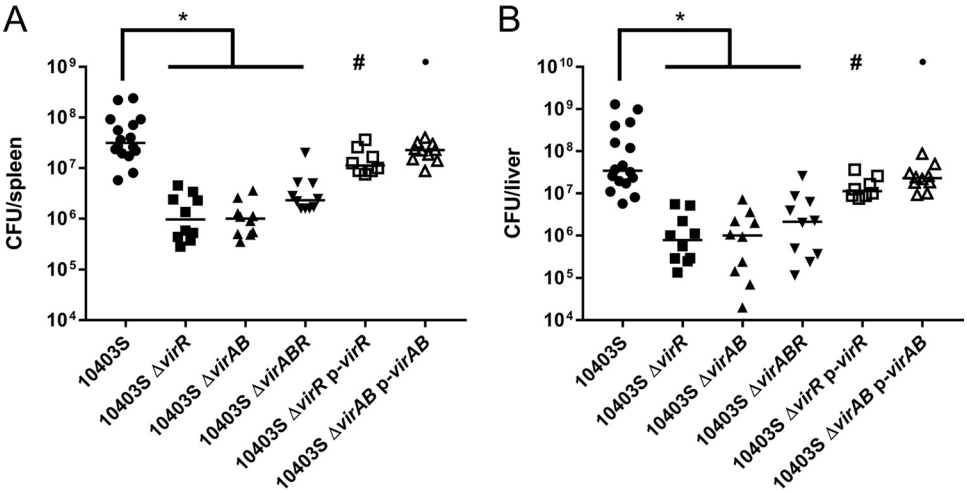

FIG 5 *In vivo* virulence of 10403S-derived strains. Eight- to 10-week-old BALB/c mice were infected via tail vein injection with 2×10^4 CFU of the indicated strains. Seventy-two hours after infection, spleens (A) and livers (B) were harvested. Harvested organs were homogenized and dilutions plated to allow the enumeration of bacteria from each organ. Each data point represents the CFU for an individual mouse. Horizontal lines indicate the median CFU for each strain. The data are compiled from three separate infection experiments with 8 to 16 mice per strain. Symbols indicate significant differences from 10403S (asterisk) ($P < 0.005$), 10403S Δ*virR* (hash tag) ($P < 0.05$), or 10403S Δ*virAB* (filled circle) ($P < 0.001$) by use of a Kruskal-Wallis test ($P < 0.0001$) with a *post hoc* Dunn multiple-comparison test.

The Δ*virAB* and Δ*virR* virulence defects could be rescued by expression of VirAB and VirR, respectively, in *trans* from an integrated vector. Taken together, these data suggest that the VirAB ABC transporter is required for the function of VirR in *L. monocytogenes* pathogenesis.

***In vitro* characterization of the virulence of 10403S Δ*virR* and 10403S Δ*virAB*.** Having established a role for VirAB in the regulation of antimicrobial resistance and *in vivo* virulence by VirR, we next sought to understand what was leading to the *in vivo* virulence and plaquing defects observed for the Δ*virR* and Δ*virAB* mutant strains. We first determined whether the virulence defects of the Δ*virR* and Δ*virAB* strains were attributable to an inherently lower growth rate of the mutant strains than of 10403S. We measured the growth of these strains in BHI broth and found no difference in growth rate between the deletion strains and 10403S (Fig. 6A). We next compared the abilities of the Δ*virR* and Δ*virAB* mutant strains to replicate inside host cells. We performed intracellular infections with the Δ*virR* and Δ*virAB* mutant strains in the L2 murine fibroblast line (Fig. 6B) and in cultured C57BL/6 bone marrow-derived macrophages (BMM) (see Fig. S1A in the supplemental material). Bacteria were recovered from host cells by lysis in 1% Triton X-100 at 2-h intervals and were plated for CFU counting. We observed no statistically significant difference in intracellular growth between the mutant strains and 10403S in either cell type. Since *virB* deletion has been shown to increase bacterial sensitivity to Triton X-100 (28), we compared the CFU counts of the Δ*virR* and Δ*virAB* strains to that of the parental strain 10403S when the strains were grown in BHI medium and were diluted in phosphate-buffered saline (PBS) alone or in PBS containing 1% Triton X-100. We observed no significant effect of Triton X-100 on bacterial viability at the concentrations and contact times used in our intracellular growth experiments (Fig. S1B). These data suggest that the plaquing defect observed for the Δ*virR* and Δ*virAB* mutants is not caused by a deficiency in growth, phagosomal escape, or intracellular replication. Since defects in *L. monocytogenes* plaquing are often attributable to a reduced ability of bacteria to spread from cell to cell during intracellular infection, we were interested in determining whether VirR is involved in ActA regulation or phosphatidylinositol-specific phospholipase C (PI-PLC) expression. While we did not observe a decrease in *actA* or *plcA* transcript levels in the Δ*virR* mutant from our RNA-seq analysis, ActA expression has been shown to be regulated posttranscriptionally (33). We therefore isolated proteins produced by 10403S, 10403S Δ*virR*, and 10403S Δ*virAB* bacteria during infection of BMM and performed Western blot analyses for ActA, PI-PLC, and the constitutively expressed p60 autolysin. These experiments showed that surface ActA (see Fig. S2A in the supplemental material) and secreted PI-PLC (Fig. S2B) protein levels in the Δ*virR* and Δ*virAB* mutant strains were similar to those in 10403S, indicating that VirR and VirAB do not significantly regulate the expression of surface ActA or secreted PI-PLC during intracellular infection.

We then determined whether the Δ*virR* and Δ*virAB* mutants exhibit defects in actin-based motility in host cells. We infected L2 cells with 10403S, 10403S Δ*virR*, or 10403S Δ*virAB*. Six hours postinfection, L2 cells were fixed with paraformaldehyde, permeabilized, and stained with anti-*L. monocytogenes* antibodies and fluorescent phalloidin to visualize F-actin filaments (Fig. 6C to E). We determined that while these three *L. monocytogenes* strains associated with F-actin to similar extents (Fig. S2C in the supplemental material), the mean lengths of the actin comet tails of the Δ*virR* and Δ*virAB* mutant strains (3.0 μm and 3.8 μm, respectively) were significantly shorter than that of strain 10403S (4.8 μm) (Fig. 6F). Since the length of the actin tail has been shown to correlate with the rate of actin-based motility (34), these data suggest that the Δ*virR* and Δ*virAB* mutants are defective in cell-to-cell spread due to a lower average movement rate of intracellular bacteria.

DISCUSSION

In this report, we have shown a previously unrecognized intracellular infection defect (plaque formation defect) for a Δ*virR* mutant of *L. monocytogenes* 10403S (Fig. 1)

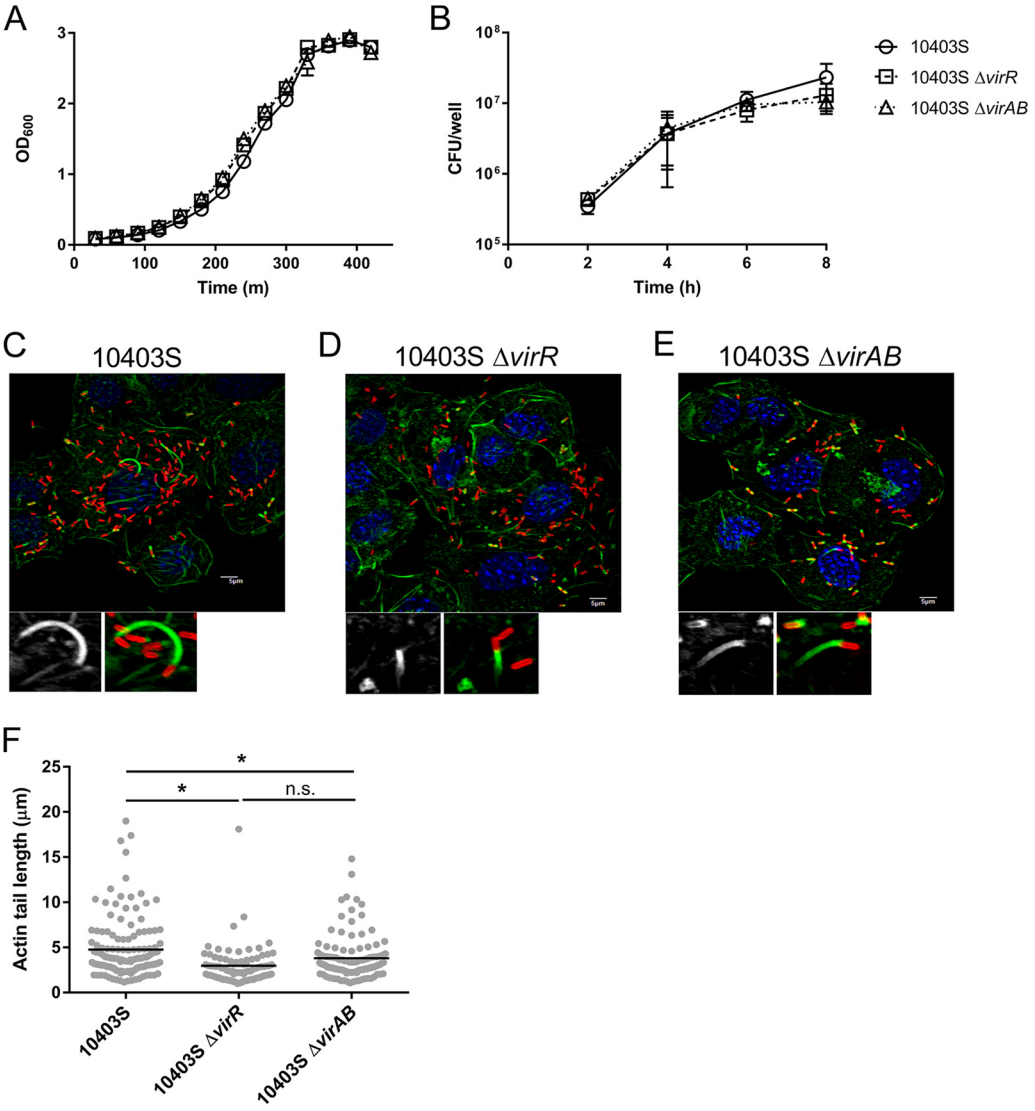

FIG 6 *In vitro* characterization of mutant strains 10403S Δ*virR* and 10403S Δ*virAB*. (A) Growth of 10403S-derived strains in BHI broth. Bacterial cultures were grown with shaking at 37°C for 7 h, and the OD_{600} was measured at 30-min intervals. Data are averages ± standard deviations for three experiments. (B) Intracellular growth in L2 murine fibroblasts. L2 fibroblasts were infected with the indicated strains. At 2-h intervals postinfection, L2 cells were lysed, and bacteria were enumerated by plating dilutions of lysates. Data are averages ± standard deviations for three experiments performed in duplicate. (C to E) Association of intracellular *L. monocytogenes* with F-actin and actin tails. L2 fibroblasts infected with the indicated strains were fixed, permeabilized, stained with anti-*L. monocytogenes* antibodies (red), phalloidin (green), and DAPI (blue), and imaged using a confocal microscope. Representative confocal images of infected L2 fibroblasts are shown. (F) Actin tail lengths. Data represent >75 measurements per strain; the mean tail length for each strain is indicated by a horizontal bar. Bacteria without actin tails were not counted. Asterisks indicate significant differences from 10403S as determined by one-way ANOVA with a *post hoc* Tukey multiple-comparison test ($P < 0.05$). n.s., not significant ($P > 0.05$).

and have also shown that the *virAB* genes, encoding a putative ABC transporter, are necessary for optimal intracellular infection and virulence (Table 2 and Fig. 5). However, the Δ*virR* and Δ*virAB* mutants did not exhibit any defects in extracellular or intracellular growth, or in the production of ActA or PI-PLC during intracellular infection (Fig. 6; also Fig. S2). This suggested that the plaquing defect of the Δ*virR* and Δ*virAB* mutants is not attributable to an inability to grow inside host cells or to a defect in vacuolar escape upon invasion. Fluorescence microscopy analyses indicated that these mutants exhibit a measureable defect in actin tail length, suggesting that the small-plaque phenotype could be a consequence of a deficiency in the rate of actin-based motility and cell-to-cell spread. Another possibility is that the Δ*virR* and Δ*virAB* mutants exhibit defects in escape

from the secondary vacuole due to misregulation of phosphatidylcholine-specific PLC (PC-PLC). While we were unable to measure PC-PLC levels in our mutant strains, it is unlikely that there is a large difference in PC-PLC expression, since the *plcB* gene is cotranscribed with *actA*.

Since the levels of surface ActA expressed by the Δ*virR* and Δ*virAB* mutants during intracellular infection were similar to that of *L. monocytogenes* 10403S, the observed defect in actin tail length is likely due to alterations of bacterial cell surface characteristics in the Δ*virR* and Δ*virAB* strains that affect optimal actin-based motility. Since the transcription of *mprF* and *dltABCD* is downregulated in the Δ*virR* mutant, the overall cell surface charge may be more negative than that of 10403S. This difference in bacterial cell surface charge could affect the charged interactions of ActA with host proteins that are necessary for actin-based motility (35, 36). While *L. monocytogenes* Δ*dltABCD* mutants have been shown previously to form actin comet tails, the length of these comet tails relative to that of wild-type *L. monocytogenes* has not been assessed (14). Interestingly, disruption of the galactosylation of wall teichoic acids has been shown to lead to shorter actin comet tails (37). Further work will be required to identify the contributions of the *dlt* operon and other individual VirR-regulated factors to *L. monocytogenes* cell-to-cell spread.

We used RNA-seq analysis to determine the *L. monocytogenes* 10403S VirR regulon (Table 1). Most of the loci identified as highly downregulated in the Δ*virR* mutant by RNA-seq were also previously identified by microarray analysis (9). These genes included the *dltABCD* operon and the *anrAB* transporter, both of which are involved in the innate resistance of *L. monocytogenes* to CAMPs. Using qRT-PCR, we confirmed that *dltD* and *anrB* transcripts were similarly downregulated in the Δ*virAB* mutant (Fig. 3). Our RNA-seq data also allowed us to identify novel members of the VirR regulon (Table 1). While most of the new loci were hypothetical proteins with <10-fold differential regulation relative to 10403S, the Rli32 sRNA was strongly regulated (~75-fold) by VirR, a finding that we then confirmed by qRT-PCR (Fig. 3C). The function of the Rli32 sRNA has yet to be investigated, but its regulation by VirR suggests that it may have roles in virulence and/or resistance to cell envelope stress that warrant further study. Furthermore, we did not observe a role for VirR in the upregulation of downstream genes in the *virR* operon, in contrast to the findings of a previous microarray analysis (9); this discrepancy is likely due to technical limitations of the initial microarray study. Taken together, these data expand our current understanding of the roles of VirR, and now VirAB, in *L. monocytogenes* gene regulation.

To further understand the relationship between VirR and VirAB, we determined the sensitivities of Δ*virR* and Δ*virAB* mutant strains to the antimicrobial agents nisin and bacitracin. We found that deletion of VirR, VirAB, or AnrB significantly reduced the MIC of nisin relative to that for 10403S, further linking the action of VirAB to VirR signaling (Table 3). It is noteworthy that our study showed a much stronger effect of *anrB* deletion on nisin sensitivity than previous reports on the AnrAB transporter (16). While we cannot directly explain this discrepancy, it may be due to differences in the *L. monocytogenes* background strains or the experimental protocols used. We also observed that growth at a high concentration of nisin led to the upregulation of the VirR-regulated genes *anrB* and *dltD* (Fig. 4). These data suggest that VirR activity increases in response to nisin. However, we were unable to show a direct role for VirR or VirAB in this upregulation, since the Δ*virR* and Δ*virAB* mutants cannot grow at the nisin concentrations necessary to observe the increase in transcript levels.

In keeping with prior data, we found that VirR and AnrB were required for *L. monocytogenes* resistance to bacitracin (16) but that VirAB is dispensable for bacitracin resistance (28). This finding suggests that under bacitracin stress, VirR signaling and thus *anrAB* expression occur in a VirAB-independent manner. It is possible that in the case of bacitracin stress, AnrAB may be the ABC transporter involved in VirR signaling. Going forward, we are interested in determining the differential roles of the two *L. monocytogenes* BceAB ABC transporter homologues, VirAB and AnrAB, in resistance to antimicrobial agents. While VirAB and AnrAB share significant sequence similarity, and

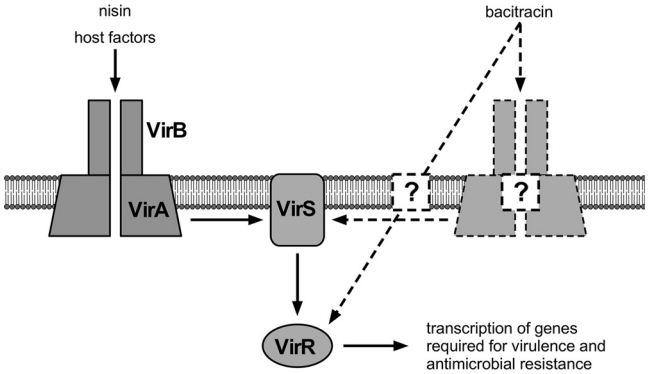

FIG 7 Model of VirABRS signaling in *L. monocytogenes*. Nisin and unknown host-derived signals are sensed by VirAB. Through interaction with VirS, VirR signaling is activated, allowing for the transcription of downstream VirR-regulated genes. The response of *L. monocytogenes* to bacitracin also depends on the action of VirR, but through a VirAB-independent mechanism. Question marks indicate that the VirAB-independent response to bacitracin could also function through an alternative ABC transporter or in a VirS-independent manner.

both are necessary for resistance to at least some antimicrobial agents, it is evident that they have evolved divergent roles in the resistance of *L. monocytogenes* to cell envelope stress. In *L. monocytogenes* 10403S, AnrAB expression is dependent on the presence of VirAB and VirR. Thus, we speculate that AnrAB likely performs a role downstream of VirAB, perhaps acting as a pump to directly export antimicrobial agents or as a transporter of bactoprenol-derived lipid, as has been suggested for BceAB (38). How the regulation of this system may work in the *L. monocytogenes* 4b G strain, where deletion of *virB* increases AnrAB expression, is as yet unclear. Studies of *virAB*, *virRS*, and *anrAB* deletion mutants will have to be performed in several strains in order to understand general coordinate regulation of these genes in *L. monocytogenes*.

We also determined the virulence phenotype of the Δ*virAB* mutant and found that it exhibited a >1-log reduction in CFU counts in the spleens and livers of infected mice (Fig. 5), like the Δ*virR* mutant. Furthermore, the Δ*virABR* strain exhibited a virulence defect that was not significantly different ($P > 0.05$) from that of either the Δ*virAB* or the Δ*virR* mutant. The lack of an additive effect on virulence from the deletion of *virAB* and *virR* supports the premise that VirAB and VirR function in the same signaling pathway with respect to virulence. However, the mechanism(s) governing the Δ*virR* and Δ*virAB* virulence defects *in vivo* remains somewhat unclear. While the cell-to-cell spread defects exhibited by the Δ*virR* and Δ*virAB* mutant strains (Fig. 1; Table 2) may contribute to the overall virulence defect phenotype *in vivo*, we do not expect that the level of reduction in cell-to-cell spread efficiency alone accounts for the >1-log reduction of bacterial burdens in organs during infection in mice (Fig. 5). One possibility is that the Δ*virR* and Δ*virAB* mutants are more susceptible to innate immune defenses than the 10403S parental strain. Previous studies of GraS, the *S. aureus* VirS homologue, have shown that the Δ*graS* strain is highly susceptible to human defensin proteins (39). It is likely that the Δ*virR* and Δ*virAB* mutants have a similar sensitivity. Such sensitivity could potentiate killing by activated innate immune cells, such as macrophages and neutrophils, *in vivo*.

Based on our data, we propose a model where VirABRS form a four-component system in which the VirAB transporter serves as the direct sensor of stress caused by host-derived factors or antimicrobial agents such as nisin (Fig. 7). How this sensing is accomplished is not immediately clear, since VirB lacks a solute binding domain, suggesting that VirAB serves as an exporter rather than an importer during translocation. While transporting its cargo, VirAB then interacts with the VirS sensor kinase, allowing for VirR activation. Once activated, VirR can induce the transcription of downstream genes necessary for pathogenesis and innate resistance to antimicrobial agents. In the case of bacitracin resistance, VirAB is not necessary, but downstream

VirR-activated genes, including *anrB*, are required for resistance. VirAB-independent activation of VirR could come from a number of sources. One possibility is that basal expression of a different ABC transporter, perhaps AnrAB, performs a role similar to that of VirAB under different stress conditions. Alternatively, VirR could be activated in a VirS-independent manner. Cross talk is occasionally observed in TCSs (40), and it is possible that one of the other 14 *L. monocytogenes* histidine kinases (41) could be activating VirR under conditions of bacitracin stress. Also, it has been shown that VirS-independent activation of VirR-regulated genes can be achieved *in vitro* by growing *L. monocytogenes* with acetate as a carbon source (9).

Since regulatory systems similar to VirABRS are widespread throughout the phylum *Firmicutes*, it has been proposed that ABC transporters like VirAB would be effective targets for antimicrobial therapy (16). Inhibitors of ABC transporters could be used to sensitize pathogenic bacteria to antibiotics to which they would otherwise display resistance. Our results show that targeted inhibitors of VirAB could have a similar effect in *L. monocytogenes* and, furthermore, would likely interfere with *L. monocytogenes* cell-to-cell spread and virulence. In conclusion, this report identifies VirAB, in addition to its known role in biofilm formation, as a new sensor required for *L. monocytogenes* pathogenesis. The requirement for VirABRS in *L. monocytogenes* virulence serves to enhance the paradigm, showing that, in addition to direct sensing of the host environment through temperature (42) or host-derived molecules (43, 44), pathogens such as *L. monocytogenes* have evolved to interpret stresses induced by host defenses as signals to undergo transcriptional changes necessary for productive infection.

MATERIALS AND METHODS

Bacterial strains. All strains used in this study are listed in Table S1 in the supplemental material. *Escherichia coli* strains were grown in lysogeny broth (also known as Luria-Bertani [LB] broth). *L. monocytogenes* strains were grown in brain heart infusion medium (BHI) (Difco, Detroit, MI) or LB broth where indicated. Bacterial stocks of strains were stored at −80°C in BHI supplemented with 20% glycerol. The following antibiotics were used at the final concentrations listed: streptomycin, 100 μg/ml; chloramphenicol, 7.5 μg/ml (*L. monocytogenes*) or 20 μg/ml (*E. coli*); gentamicin, 5 to 30 μg/ml; and ampicillin, 100 μg/ml (Sigma-Aldrich, St. Louis, MO).

Cell culture. Bone marrow-derived macrophages (BMM) were isolated as described previously (45). Briefly, 8- to 12-week-old C57BL/6 mice (The Jackson Laboratory, Bar Harbor, ME) were euthanized and their femurs removed. Bone marrow was then flushed from the femurs with Dulbecco's modified Eagle's medium (DMEM) (Mediatech, Manassas, VA) supplemented with 10% fetal bovine serum (FBS) (HyClone, Logan, UT), 4.5 g/liter glucose, 2 mM glutamine, 1 mM sodium pyruvate, and 100 μg/ml penicillin-streptomycin (P-S). Cells were then cultured in DMEM supplemented with 10% FBS, 2 mM glutamine, 1 mM sodium pyruvate, 100 μg/ml P-S, 55 μM β-mercaptoethanol, and 30% L-cell conditioned medium in 150-mm non-tissue culture-treated petri dishes (Nalge Nunc International, Rochester, NY). On day 3, fresh BMM medium was added to the cultures. On day 6, the medium was removed from the cells, and BMM were harvested. BMM were then plated in antibiotic-free medium 18 to 24 h prior to experiments as indicated. Mouse L2 fibroblasts were grown in RPMI 1640 medium (Mediatech, Manassas, VA) supplemented with 10% FBS, 2 mM glutamine, 1 mM sodium pyruvate, and 100 μg/ml P-S. All cells were cultured at 37°C under a 5% CO_2 atmosphere.

Plasmid and strain construction. All plasmids used in this study are listed in Table S1, and all primers used in this study are listed in Table S2, in the supplemental material. In-frame deletion alleles were produced using splicing by overlap extension PCR as described previously (46). The resulting PCR products were ligated into pKSV7 (47) using the PstI/SalI sites in the case of the Δ*virR*, Δ*virAB*, and Δ*virABR* deletions to generate pKSV7 Δ*virR*, pKSV7 Δ*virAB*, and pKSV7 Δ*virABR*, respectively. In the case of the Δ*anrB* deletion, PCR products were ligated into pCON1 (48) using HindIII and SalI sites to generate pCON1 Δ*anrB*. The pKSV7-based plasmids were electroporated into 10403S, and allelic exchange was performed as described previously (49) to generate strains DH-L2111, DH-L2113, and DH-L2115, respectively. pCON1 Δ*anrB* was electroporated into *E. coli* SM10 and was then introduced into 10403S through conjugation as described previously (50, 51). Allelic exchange was then performed in the same manner as for the other strains to generate strain DH-L2116. Complementing vectors were constructed by amplifying the *virR* and *virAB* open reading frames and ligating the PCR products into pLOV (30) using SalI/KpnI restriction sites to generate pLOV::*virR* and p-*virAB*, respectively. These plasmids were electroporated into *E. coli* SM10 and were then introduced into DH-L2113 via conjugation to produce strains DH-L2143 and DH-L2114. The p-*virR* complementing vector was generated by amplifying the *virR* promoter and open reading frame and ligating this product into pPL3 (52). The p-*virR* vector was introduced into DH-L2111 using conjugation to generate strain DH-L2144. PCRs were performed using *PfuTurbo* DNA polymerase AD (Agilent, Wilmington, DE) according to the manufacturer's instructions.

Plaquing analysis. A total of 2×10^6 L2 mouse fibroblasts were seeded per well of a 6-well plate and were grown in RPMI medium with 10% serum for 18 to 24 h. *L. monocytogenes* strains were grown

for 18 to 24 h in BHI with streptomycin at 30°C without shaking. Two microliters of a 1:10 dilution of the 18- to 24-h bacterial culture was added to the L2 cells in RPMI medium. The infected L2 cells were incubated for 1 h at 37°C in a tissue culture incubator. Infected cells were then washed twice in PBS and overlaid with DMEM containing 5% serum, 0.7% agarose, and 30 μg/ml gentamicin. Cells were then incubated for 3 days to allow plaques to form, and a second overlay of agarose and DMEM containing 200 μg/ml neutral red and 12 mM HCl was added. Twenty-four hours later, plaques were imaged, and the relative plaque diameters were measured using Adobe Photoshop.

Gene expression analysis by RNA sequencing. Strains were grown in BHI with streptomycin for 20 h at 37°C with shaking. Bacteria were then washed with PBS and were diluted 1:100 into LB with streptomycin. Bacteria were grown for 3.5 h at 37°C with shaking, and samples were pelleted. RNA was extracted from samples using a FastPrep RNApro solution and lysing matrix B (MP Biomedicals, Santa Ana, CA) according to the manufacturer's instructions. The isolated RNA was submitted to the Harvard Medical School Biopolymers Facility for rRNA reduction, library preparation, and sequencing. rRNA was removed from the samples using the Ribo-Zero rRNA removal kit for Gram-positive bacteria (Illumina, San Diego, CA). Samples were prepared for strand-specific RNA sequencing using the PrepX RNA-Seq library kit (Wafergen, Fremont, CA) according to the manufacturer's instructions. Samples were multiplexed and were run in duplicate on two separate lanes of a flow cell using an Illumina HiSeq 2500 system. Data were analyzed using the CLC Bio Genomics Workbench, version 7.5.1. Reads were mapped to the *L. monocytogenes* 10403S (NC_017544.1) and EGD-e (NC_003210.1) genomes. Only reads that mapped to non-rRNA features were counted to account for differences in rRNA reduction effectiveness between samples. Differential expression was determined using the "Exact Test" for two-group comparisons (53) as implemented in CLC Genomics Workbench. The differential expression data presented include all features significantly ($P < 0.01$) differentially expressed at least 2-fold. Multiple-hypothesis testing was corrected for by using the false-discovery rate (FDR).

MIC determination. MICs of nisin and bacitracin were determined as described previously (54). Briefly, serial 2-fold dilutions of the antibiotic of interest were made in 100 μl of BHI with streptomycin in a 96-well microtiter plate. An *L. monocytogenes* strain was then added to each well in 100 μl of BHI with streptomycin at a final concentration of 10^5 CFU/ml. Plates were incubated for 20 h at 37°C, and then the optical density at 600 nm (OD_{600}) was read using a SpectraMax spectrophotometer (Molecular Devices, Sunnyvale, CA). The MIC was defined as the minimum concentration of antibiotic that led to no detectable growth of the strain. Data presented are averages from three separate experiments performed in duplicate.

***In vivo* virulence analysis.** *In vivo* infections were performed as described previously (55). Briefly, strains were grown for 16 to 18 h at 30°C in BHI with streptomycin without shaking. Eight- to 10-week-old female BALB/c mice (The Jackson Laboratory, Bar Harbor, ME) were injected intravenously with 1.7×10^4 to 2.4×10^4 CFU of each strain. Seventy-two hours after infection, the mice were sacrificed, and livers and spleens were homogenized in 5 ml of PBS. Bacterial burdens in each organ were enumerated by plating dilutions of the organ homogenates on LB agar with streptomycin plates and incubating the plates for 48 h at 37°C. All animal studies were performed according to IACUC regulations.

Gene expression analysis by quantitative PCR. Cultures of the strains were grown for 20 h in BHI with streptomycin at 37°C with shaking. The following day, the cultures were diluted 1:100 into fresh BHI containing streptomycin. Nisin was added to certain cultures as indicated. Cultures were incubated at 37°C with shaking until the OD_{600} reached 0.4 to 0.6. The cultures were collected by centrifugation, and RNA was isolated using a FastPrep RNApro solution and lysing matrix B (MP Biomedicals, Santa Ana, CA) according to the manufacturer's instructions. The isolated RNA was then reverse transcribed and amplified using a Step One Plus thermocycler (Applied Biosystems, Waltham, MA) and a QuantiTect SYBR green RT-PCR kit (Qiagen, Valencia, CA).

***In vitro* growth analysis.** Twenty-hour cultures of the strains were diluted 1:50 into BHI in triplicate flasks and were grown with shaking at 37°C. The OD_{600} was measured at 30-min intervals, and values were averaged across the triplicate samples.

Intracellular growth analysis. Strains were grown for 20 h in BHI with streptomycin at 30°C without shaking. A total of 5×10^5 host cells, either C57BL/6 mouse BMM or L2 mouse fibroblasts, were seeded into each well of a 24-well plate and were incubated in appropriate media for 20 h. After incubation, the bacteria were collected by centrifugation, washed twice with PBS, and added to the host cells in DMEM at a multiplicity of infection (MOI) of 50 (L2 fibroblasts) or 1 (BMM). One hour after infection, infected cells were washed with PBS, and DMEM containing 5 μg/ml gentamicin was added to the infected cells. At various time intervals, bacteria were collected by lysing host cells in PBS containing 1% Triton X-100. Dilutions of the lysates were then plated on BHI agar with streptomycin plates and were incubated for 18 to 24 h at 37°C to enumerate CFU.

Intracellular ActA and PI-PLC expression analysis. *L. monocytogenes* strains were grown for 20 h in BHI with streptomycin at 30°C without shaking. A total of 1×10^6 BMM were seeded into each well of a 12-well plate and were grown in BMM growth medium for 20 h in a tissue culture incubator at 37°C. The BMM medium was then removed and replaced with fresh BMM medium containing 1×10^7 CFU *L. monocytogenes*. One hour after infection, the medium was removed, the infected cells were washed twice with PBS, and fresh BMM medium plus 5 μg/ml gentamicin was added back. Four hours after infection, the medium was removed, and the infected host cells were lysed in 150 μl SDS sample buffer (0.25 M Tris-HCl [pH 6.8], 10% sodium dodecyl sulfate, 50% glycerol, 0.5 M dithiothreitol, 0.25% bromophenol blue). The resulting lysates were heated at 95°C and were then run on an 8% (ActA and p60) or 14% (PI-PLC and p60) SDS-PAGE gel. The gels were blotted onto polyvinylidene difluoride (PVDF) membranes, which were then cut, blocked, and probed with anti-ActA (rabbit polyclonal), anti-PI-PLC

(rabbit polyclonal), or anti-p60 (mouse monoclonal) (Adipogen, San Diego, CA) antibodies. Blots were washed in Tris-buffered saline with Tween (TBST) and were then reprobed with anti-rabbit or anti-mouse antibodies conjugated to horseradish peroxidase (Cell Signaling Technologies, Danvers, MA). The blots were then incubated in SuperSignal West Pico chemiluminescent substrate (Thermo Fisher, Waltham, MA) and were imaged using an Amersham 600 imager (GE, Boston, MA).

Confocal microscopy of infected cells. L2 mouse fibroblasts were seeded in RPMI medium at 7.5×10^5/well in a 6-well plate containing a coverslip and were incubated for 20 h in a tissue culture incubator at 37°C. *L. monocytogenes* strains were grown at 30°C without shaking for 20 h in BHI with streptomycin. Cultures were washed in PBS, and L2 cells were infected with bacteria at an MOI of 50. One hour postinfection, L2 cells were washed with PBS, and fresh RPMI medium with 5 μg/ml gentamicin was added to each well. Six hours postinfection, coverslips were washed with PBS and were fixed in 4% paraformaldehyde for 15 min at room temperature (25°C). Coverslips were washed with PBS, permeabilized with 0.5% Triton X-100 for 5 min, and prepared for fluorescence microscopy. Coverslips were blocked with 3% (wt/vol) bovine serum albumin (BSA) in PBS and were incubated with a rabbit polyclonal antibody against *L. monocytogenes* (BD Difco, Franklin Lakes, NJ). Coverslips were then rinsed with PBS and were treated with an Alexa Fluor 647-conjugated donkey anti-rabbit IgG antibody (Jackson ImmunoResearch, West Grove, PA) and Alexa Fluor 488-conjugated phalloidin (Molecular Probes, Eugene, OR) together with 4′,6-diamidino-2-phenylindole (DAPI) for labeling nuclei. Specimens were mounted for microscopy using PermaFluor mounting medium (Thermo Fisher, Waltham, MA) and were analyzed by fluorescence microscopy. Confocal images were acquired with a FluoView FV1000 microscope (Olympus, Tokyo, Japan) with a 60× oil immersion objective lens and were processed with FluoView software (Olympus, Tokyo, Japan). NIH ImageJ software was used to quantify *L. monocytogenes* cells, as well as *L. monocytogenes* cells associated with F-actin, and to measure the length of each F-actin comet tail in each image. F-actin tails were defined as being phalloidin positive and >1 μm in length.

Accession number(s). RNA-seq data are available in the Gene Expression Omnibus database under series record GSE98373.

SUPPLEMENTAL MATERIAL

Supplemental material for this article may be found at https://doi.org/10.1128/IAI.00901-17.

SUPPLEMENTAL FILE 1, PDF file, 0.8 MB.

ACKNOWLEDGMENTS

This work was supported by U.S. Public Health Service grant AI53669 from the National Institutes of Health (to D.E.H.) and Sponsored Research Funding from Aduro Biotech, Inc. We do not have any conflicts of interest related to the results or interpretation of the information presented in this work.

REFERENCES

1. Vázquez-Boland JA, Kuhn M, Berche P, Chakraborty T, Dominguez-Bernal G, Goebel W, Gonzalez-Zorn B, Wehland J, Kreft J. 2001. *Listeria* pathogenesis and molecular virulence determinants. Clin Microbiol Rev 14:584–640. https://doi.org/10.1128/CMR.14.3.584-640.2001.
2. Freitag NE, Port GC, Miner MD. 2009. *Listeria monocytogenes*—from saprophyte to intracellular pathogen. Nat Rev Microbiol 7:623–628. https://doi.org/10.1038/nrmicro2171.
3. Toledo-Arana A, Dussurget O, Nikitas G, Sesto N, Guet-Revillet H, Balestrino D, Loh E, Gripenland J, Tiensuu T, Vaitkevicius K, Barthelemy M, Vergassola M, Nahori MA, Soubigou G, Regnault B, Coppee JY, Lecuit M, Johansson J, Cossart P. 2009. The *Listeria* transcriptional landscape from saprophytism to virulence. Nature 459:950–956. https://doi.org/10.1038/nature08080.
4. Scortti M, Monzo HJ, Lacharme-Lora L, Lewis DA, Vázquez-Boland JA. 2007. The PrfA virulence regulon. Microbes Infect 9:1196–1207. https://doi.org/10.1016/j.micinf.2007.05.007.
5. Lambrechts A, Gevaert K, Cossart P, Vandekerckhove J, Van Troys M. 2008. *Listeria* comet tails: the actin-based motility machinery at work. Trends Cell Biol 18:220–227. https://doi.org/10.1016/j.tcb.2008.03.001.
6. Ollinger J, Bowen B, Wiedmann M, Boor KJ, Bergholz TM. 2009. *Listeria monocytogenes* σ^B modulates PrfA-mediated virulence factor expression. Infect Immun 77:2113–2124. https://doi.org/10.1128/IAI.01205-08.
7. Lobel L, Sigal N, Borovok I, Belitsky BR, Sonenshein AL, Herskovits AA. 2015. The metabolic regulator CodY links *Listeria monocytogenes* metabolism to virulence by directly activating the virulence regulatory gene *prfA*. Mol Microbiol 95:624–644. https://doi.org/10.1111/mmi.12890.
8. Lobel L, Sigal N, Borovok I, Ruppin E, Herskovits AA. 2012. Integrative genomic analysis identifies isoleucine and CodY as regulators of *Listeria monocytogenes* virulence. PLoS Genet 8:e1002887. https://doi.org/10.1371/journal.pgen.1002887.
9. Mandin P, Fsihi H, Dussurget O, Vergassola M, Milohanic E, Toledo-Arana A, Lasa I, Johansson J, Cossart P. 2005. VirR, a response regulator critical for *Listeria monocytogenes* virulence. Mol Microbiol 57:1367–1380. https://doi.org/10.1111/j.1365-2958.2005.04776.x.
10. Williams RH, Whitworth DE. 2010. The genetic organisation of prokaryotic two-component system signalling pathways. BMC Genomics 11:720. https://doi.org/10.1186/1471-2164-11-720.
11. Stock AM, Robinson VL, Goudreau PN. 2000. Two-component signal transduction. Annu Rev Biochem 69:183–215. https://doi.org/10.1146/annurev.biochem.69.1.183.
12. Camejo A, Buchrieser C, Couve E, Carvalho F, Reis O, Ferreira P, Sousa S, Cossart P, Cabanes D. 2009. *In vivo* transcriptional profiling of *Listeria monocytogenes* and mutagenesis identify new virulence factors involved in infection. PLoS Pathog 5:e1000449. https://doi.org/10.1371/journal.ppat.1000449.
13. Perego M, Glaser P, Minutello A, Strauch MA, Leopold K, Fischer W. 1995. Incorporation of D-alanine into lipoteichoic acid and wall teichoic acid in *Bacillus subtilis*. Identification of genes and regulation. J Biol Chem 270:15598–15606.
14. Abachin E, Poyart C, Pellegrini E, Milohanic E, Fiedler F, Berche P, Trieu-Cuot P. 2002. Formation of D-alanyl-lipoteichoic acid is required for adhesion and virulence of *Listeria monocytogenes*. Mol Microbiol 43:1–14. https://doi.org/10.1046/j.1365-2958.2002.02723.x.
15. Thedieck K, Hain T, Mohamed W, Tindall BJ, Nimtz M, Chakraborty T, Wehland J, Jansch L. 2006. The MprF protein is required for lysinylation of phospholipids in listerial membranes and confers resistance to cationic

antimicrobial peptides (CAMPs) on *Listeria monocytogenes*. Mol Microbiol 62:1325–1339. https://doi.org/10.1111/j.1365-2958.2006.05452.x.
16. Collins B, Curtis N, Cotter PD, Hill C, Ross RP. 2010. The ABC transporter AnrAB contributes to the innate resistance of *Listeria monocytogenes* to nisin, bacitracin, and various beta-lactam antibiotics. Antimicrob Agents Chemother 54:4416–4423. https://doi.org/10.1128/AAC.00503-10.
17. Kang J, Wiedmann M, Boor KJ, Bergholz TM. 2015. VirR-mediated resistance of *Listeria monocytogenes* against food antimicrobials and cross-protection induced by exposure to organic acid salts. Appl Environ Microbiol 81:4553–4562. https://doi.org/10.1128/AEM.00648-15.
18. Ohki R, Giyanto Tateno K, Masuyama W, Moriya S, Kobayashi K, Ogasawara N. 2003. The BceRS two-component regulatory system induces expression of the bacitracin transporter, BceAB, in *Bacillus subtilis*. Mol Microbiol 49:1135–1144. https://doi.org/10.1046/j.1365-2958.2003.03653.x.
19. Coumes-Florens S, Brochier-Armanet C, Guiseppi A, Denizot F, Foglino M. 2011. A new highly conserved antibiotic sensing/resistance pathway in Firmicutes involves an ABC transporter interplaying with a signal transduction system. PLoS One 6:e15951. https://doi.org/10.1371/journal.pone.0015951.
20. Dintner S, Staron A, Berchtold E, Petri T, Mascher T, Gebhard S. 2011. Coevolution of ABC transporters and two-component regulatory systems as resistance modules against antimicrobial peptides in *Firmicutes* bacteria. J Bacteriol 193:3851–3862. https://doi.org/10.1128/JB.05175-11.
21. Falord M, Karimova G, Hiron A, Msadek T. 2012. GraXSR proteins interact with the VraFG ABC transporter to form a five-component system required for cationic antimicrobial peptide sensing and resistance in *Staphylococcus aureus*. Antimicrob Agents Chemother 56:1047–1058. https://doi.org/10.1128/AAC.05054-11.
22. Dintner S, Heermann R, Fang C, Jung K, Gebhard S. 2014. A sensory complex consisting of an ATP-binding cassette transporter and a two-component regulatory system controls bacitracin resistance in *Bacillus subtilis*. J Biol Chem 289:27899–27910. https://doi.org/10.1074/jbc.M114.596221.
23. Bernard R, Guiseppi A, Chippaux M, Foglino M, Denizot F. 2007. Resistance to bacitracin in *Bacillus subtilis*: unexpected requirement of the BceAB ABC transporter in the control of expression of its own structural genes. J Bacteriol 189:8636–8642. https://doi.org/10.1128/JB.01132-07.
24. Bécavin C, Bouchier C, Lechat P, Archambaud C, Creno S, Gouin E, Wu Z, Kuhbacher A, Brisse S, Pucciarelli MG, Garcia-del Portillo F, Hain T, Portnoy DA, Chakraborty T, Lecuit M, Pizarro-Cerda J, Moszer I, Bierne H, Cossart P. 2014. Comparison of widely used *Listeria monocytogenes* strains EGD, 10403S, and EGD-e highlights genomic variations underlying differences in pathogenicity. mBio 5:e00969-14. https://doi.org/10.1128/mBio.00969-14.
25. Burke TP, Portnoy DA. 2016. SpoVG is a conserved RNA-binding protein that regulates *Listeria monocytogenes* lysozyme resistance, virulence, and swarming motility. mBio 7:e00240. https://doi.org/10.1128/mBio.00240-16.
26. Quereda JJ, Ortega AD, Pucciarelli MG, Garcia-Del Portillo F. 2014. The *Listeria* small RNA *rli27* regulates a cell wall protein inside eukaryotic cells by targeting a long 5′-UTR variant. PLoS Genet 10:e1004765. https://doi.org/10.1371/journal.pgen.1004765.
27. Suo Y, Huang Y, Liu Y, Shi C, Shi X. 2012. The expression of superoxide dismutase (SOD) and a putative ABC transporter permease is inversely correlated during biofilm formation in *Listeria monocytogenes* 4b G. PLoS One 7:e48467. https://doi.org/10.1371/journal.pone.0048467.
28. Zhu X, Long F, Chen Y, Knochel S, She Q, Shi X. 2008. A putative ABC transporter is involved in negative regulation of biofilm formation by *Listeria monocytogenes*. Appl Environ Microbiol 74:7675–7683. https://doi.org/10.1128/AEM.01229-08.
29. Zhu X, Liu W, Lametsch R, Aarestrup F, Shi C, She Q, Shi X, Knochel S. 2011. Phenotypic, proteomic, and genomic characterization of a putative ABC-transporter permease involved in *Listeria monocytogenes* biofilm formation. Foodborne Pathog Dis 8:495–501. https://doi.org/10.1089/fpd.2010.0697.
30. Higgins DE, Buchreiser C, Freitag NE. 2006. Genetic tools for use with *Listeria monocytogenes*, p 620–623. *In* Fischetti VA, Novick RP, Ferretti JJ, Portnoy DA, Rood JI (ed), Gram-positive pathogens, 2nd ed. ASM Press, Washington, DC.
31. Breukink E, Wiedemann I, van Kraaij C, Kuipers OP, Sahl HG, de Kruijff B. 1999. Use of the cell wall precursor lipid II by a pore-forming peptide antibiotic. Science 286:2361–2364. https://doi.org/10.1126/science.286.5448.2361.
32. Stone KJ, Strominger JL. 1971. Mechanism of action of bacitracin: complexation with metal ion and C_{55}-isoprenyl pyrophosphate. Proc Natl Acad Sci U S A 68:3223–3227. https://doi.org/10.1073/pnas.68.12.3223.
33. Wong KK, Bouwer HG, Freitag NE. 2004. Evidence implicating the 5′ untranslated region of *Listeria monocytogenes actA* in the regulation of bacterial actin-based motility. Cell Microbiol 6:155–166. https://doi.org/10.1046/j.1462-5822.2003.00348.x.
34. Theriot JA, Mitchison TJ, Tilney LG, Portnoy DA. 1992. The rate of actin-based motility of intracellular *Listeria monocytogenes* equals the rate of actin polymerization. Nature 357:257–260. https://doi.org/10.1038/357257a0.
35. Skoble J, Portnoy DA, Welch MD. 2000. Three regions within ActA promote Arp2/3 complex-mediated actin nucleation and *Listeria monocytogenes* motility. J Cell Biol 150:527–538. https://doi.org/10.1083/jcb.150.3.527.
36. Lauer P, Theriot JA, Skoble J, Welch MD, Portnoy DA. 2001. Systematic mutational analysis of the amino-terminal domain of the *Listeria monocytogenes* ActA protein reveals novel functions in actin-based motility. Mol Microbiol 42:1163–1177. https://doi.org/10.1046/j.1365-2958.2001.02677.x.
37. Spears PA, Havell EA, Hamrick TS, Goforth JB, Levine AL, Abraham ST, Heiss C, Azadi P, Orndorff PE. 2016. *Listeria monocytogenes* wall teichoic acid decoration in virulence and cell-to-cell spread. Mol Microbiol 101:714–730. https://doi.org/10.1111/mmi.13353.
38. Kingston AW, Zhao H, Cook GM, Helmann JD. 2014. Accumulation of heptaprenyl diphosphate sensitizes *Bacillus subtilis* to bacitracin: implications for the mechanism of resistance mediated by the BceAB transporter. Mol Microbiol 93:37–49. https://doi.org/10.1111/mmi.12637.
39. Kraus D, Herbert S, Kristian SA, Khosravi A, Nizet V, Gotz F, Peschel A. 2008. The GraRS regulatory system controls *Staphylococcus aureus* susceptibility to antimicrobial host defenses. BMC Microbiol 8:85. https://doi.org/10.1186/1471-2180-8-85.
40. Laub MT, Goulian M. 2007. Specificity in two-component signal transduction pathways. Annu Rev Genet 41:121–145. https://doi.org/10.1146/annurev.genet.41.042007.170548.
41. Glaser P, Frangeul L, Buchrieser C, Rusniok C, Amend A, Baquero F, Berche P, Bloecker H, Brandt P, Chakraborty T, Charbit A, Chetouani F, Couve E, de Daruvar A, Dehoux P, Domann E, Dominguez-Bernal G, Duchaud E, Durant L, Dussurget O, Entian KD, Fsihi H, Garcia-del Portillo F, Garrido P, Gautier L, Goebel W, Gomez-Lopez N, Hain T, Hauf J, Jackson D, Jones LM, Kaerst U, Kreft J, Kuhn M, Kunst F, Kurapkat G, Madueno E, Maitournam A, Vicente JM, Ng E, Nedjari H, Nordsiek G, Novella S, de Pablos B, Perez-Diaz JC, Purcell R, Remmel B, Rose M, Schlueter T, Simoes N, et al. 2001. Comparative genomics of *Listeria* species. Science 294:849–852. https://doi.org/10.1126/science.1063447.
42. Leimeister-Wächter M, Domann E, Chakraborty T. 1992. The expression of virulence genes in *Listeria monocytogenes* is thermoregulated. J Bacteriol 174:947–952. https://doi.org/10.1128/jb.174.3.947-952.1992.
43. Reniere ML, Whiteley AT, Hamilton KL, John SM, Lauer P, Brennan RG, Portnoy DA. 2015. Glutathione activates virulence gene expression of an intracellular pathogen. Nature 517:170–173. https://doi.org/10.1038/nature14029.
44. Haber A, Friedman S, Lobel L, Burg-Golani T, Sigal N, Rose J, Livnat-Levanon N, Lewinson O, Herskovits AA. 2017. L-Glutamine induces expression of *Listeria monocytogenes* virulence genes. PLoS Pathog 13:e1006161. https://doi.org/10.1371/journal.ppat.1006161.
45. Alberti-Segui C, Goeden KR, Higgins DE. 2007. Differential function of *Listeria monocytogenes* listeriolysin O and phospholipases C in vacuolar dissolution following cell-to-cell spread. Cell Microbiol 9:179–195. https://doi.org/10.1111/j.1462-5822.2006.00780.x.
46. Horton RM, Hunt HD, Ho SN, Pullen JK, Pease LR. 1989. Engineering hybrid genes without the use of restriction enzymes: gene splicing by overlap extension. Gene 77:61–68. https://doi.org/10.1016/0378-1119(89)90359-4.
47. Smith K, Youngman P. 1992. Use of a new integrational vector to investigate compartment-specific expression of the *Bacillus subtilis spoIIM* gene. Biochimie 74:705–711. https://doi.org/10.1016/0300-9084(92)90143-3.
48. Behari J, Youngman P. 1998. Regulation of *hly* expression in *Listeria monocytogenes* by carbon sources and pH occurs through separate mechanisms mediated by PrfA. Infect Immun 66:3635–3642.
49. Camilli A, Tilney LG, Portnoy DA. 1993. Dual roles of *plcA* in *Listeria monocytogenes* pathogenesis. Mol Microbiol 8:143–157. https://doi.org/10.1111/j.1365-2958.1993.tb01211.x.

50. Simon R, Priefer U, Pühler A. 1983. A broad host range mobilization system for *in vivo* genetic engineering: transposon mutagenesis in Gram negative bacteria. Nat Biotechnol 1:784–791. https://doi.org/10.1038/nbt1183-784.
51. Barák I, Behari J, Olmedo G, Guzman P, Brown DP, Castro E, Walker D, Westpheling J, Youngman P. 1996. Structure and function of the *Bacillus* SpoIIE protein and its localization to sites of sporulation septum assembly. Mol Microbiol 19:1047–1060. https://doi.org/10.1046/j.1365-2958.1996.433963.x.
52. Shen A, Higgins DE. 2005. The 5′ untranslated region-mediated enhancement of intracellular listeriolysin O production is required for *Listeria monocytogenes* pathogenicity. Mol Microbiol 57:1460–1473. https://doi.org/10.1111/j.1365-2958.2005.04780.x.
53. Robinson MD, Smyth GK. 2008. Small-sample estimation of negative binomial dispersion, with applications to SAGE data. Biostatistics 9:321–332. https://doi.org/10.1093/biostatistics/kxm030.
54. Wiedemann I, Bottiger T, Bonelli RR, Wiese A, Hagge SO, Gutsmann T, Seydel U, Deegan L, Hill C, Ross P, Sahl HG. 2006. The mode of action of the lantibiotic lacticin 3147—a complex mechanism involving specific interaction of two peptides and the cell wall precursor lipid II. Mol Microbiol 61:285–296. https://doi.org/10.1111/j.1365-2958.2006.05223.x.
55. Portnoy DA, Jacks PS, Hinrichs DJ. 1988. Role of hemolysin for the intracellular growth of *Listeria monocytogenes*. J Exp Med 167:1459–1471. https://doi.org/10.1084/jem.167.4.1459.